Proc. SPIE Vol. **5912**, ISBN 0-8194-5917-8, pp. 129 - 128 (2005).

Solid-State Molecular Sensors (SSMS) based on confined III-IV-V_2 multi-functional heterostructures

Nikolaus Dietz,[*a] Frank Madarasz,[b] and Ramarao Inguva[b]
[a] Department of Physics and Astronomy, Georgia State University, Atlanta, GA 30302
[b] East West Enterprises, Inc., Huntsville, AL 35816

ABSTRACT

Nonlinear confined (optical and/or electrical) heterostructures based on III-IV-V_2 chalcopyrite (CP) thin films and/or embedded CP materials offer unique advantages over group III-V and IV linear structures. These stem from the birefringent nature and the lower crystal symmetry of the CP semiconductors. As an example, this property is responsible three-wave nonlinear parametric processes (a second-order nonlinear effect) and very high values of the second-order hyperpolarizabilities. The recent discovery of room-temperature ferromagnetism in diluted magnetic CP semiconductors adds an additional functionality to this material system that makes possible the construction of novel magneto-optical device structures based on ferromagnetic nanocomposites and confined ferromagnetic heterostructures, which can be embedded in confined birefringent layers. Such structures are the basic elements for advanced "Solid-State Molecular Sensor" (SSMS) device structures. Rugged, *miniaturized* SSMS structures can be constructed which are based on a unique, optically confined birefringent, group II-IV-V_2 CP heterostructure technology. This system identifies target chemicals and biological molecules in *real-time* under ambient conditions. It can detect and discriminate between numerous and varied molecular species by employing resonant phase- and/or amplitude sensitive detection over a large, tunable spectral range. The SSMS can be made sensitive to a specific group of molecules with appropriate phase matching conditions. Its response is unlike that of a linear waveguide sensor in two primary areas: change of frequency output, and intensity of the output light generated. Both signals are generated in a nonlinear second harmonic generation process sensitive to small changes in the phase matching conditions. Potential applications include compact ultra-sensitive sensors, nonlinear optical modulators, magnetic photonic crystals, magneto-optical switches, detectors, and spin electronic devices.

Keywords: Solid state molecular sensor, chalcopyrite thin film, wave guided structures, nonlinear wave guides

1. INTRODUCTION

The need for a rugged, miniaturized sensor to detect, discriminate, and quantify these and other target chemical/biological (CB) agents in real time is crucial and of high priority. The proposed, highly integrated technology - Solid State Molecular Sensor (SSMS) and variants, along with SSMS networks—fits these critical operational criteria. The principles of the SSMS system have been worked out in detail and are the subject matter of two patents.[1,2] A third patent,[3] which is spintronics version, is pending. In addition, the technology is supported by two relatively recent publications.[4,5]

Presently, several optical detection concepts are being explored utilizing optical fibers and linear waveguided structures. A review of the various techniques has been provided by Boisdé et al.[6] Each have a niche market for a specific application. Most, however, lack the potential for further development due to limitations either in sensitivity, integration, handling, or discrimination capabilities. The essential criteria that must be considered in the development of a compact, integrated CB detection system are summarized in Table 1 and focus on localized detection.

These criteria are different from the applications requirements that mandate probing over large distances/volumes. In this case, integration is less important, and the key technological task is the development of high-intensity lasers operating at wavelengths in the mid- (3-5 microns) and far-IR (8-12 microns).[7-11] The limitations imposed by the

[*] Email: ndietz@gsu.edu

transparency windows of the earth's atmosphere in such high power applications fortunately do not apply to the highly localized SSMS systems, which generally provides for a wider range of detection. In the development of compact, highly integrated SSMS systems it is necessary to keep in mind that substantial *initial efforts must be made that focus on materials, device structure design, simulations and validation of performance to demonstrate feasibility of a SSMS network*.

Table 1: Criteria for compact, integrated CB detection systems

1) ***high sensitivity /low detection limits***
2) ***simultaneous detection and discrimination of CB agents***
3) ***self-calibration and adjustable warning and alarm level functions***
4) ***robust maintenance and easy exchangeable modules***
5) ***operational at normal environmental conditions***
6) ***low power consumption***
7) ***functional reliability/long life***
8) ***portability.***

The SSMS concept is based on birefringent and/or magnetic, optically confined nonlinear chalcopyrite (CP) heterostructures. It differs significantly from conventional waveguide sensors as is clearly illustrated in the patents[1-3] cited earlier in the paper. In a conventional waveguide sensor, changes in the evanescent wave (phase- and/or amplitude) are analyzed either interferometrically (phase shift) or by integral means (absorption loss). The SSMS concept uses a nonlinear, birefringent medium to translate phase and amplitude changes in the evanescent wave - during an optical parametric oscillator (OPO) process - in frequency shift, that can be detected with high accuracy. Its operational process is unique and to our knowledge as never been exploited by any other optical sensor system.

Such a detection system has the advantage that it can utilize conventional, well-established semiconductor lasers that emit in the visible or near infrared wavelength range with no cooling requirements. The useful transparency region of single- and/or multiple layered, nonlinear, waveguided chalcopyrite heterostructure(s) extends from the visible to far-IR wavelength regime depending on the chalcopyrite compounds chosen. That is, approximately in the range of 0.6 μm through 20 μm. The wavelength tunability in these CP heterostructures allows for the discrimination and identification of almost all molecular structures in a probed medium or attached at a probed interface/surface, using resonant phase- and/or amplitude sensitive detection.

2. DEVELOPMENT OF SOLID-STATE MOLECULAR SENSOR (SSMS)

2.1. SSMS components

Figure 1 shows the development steps leading to a Solid-State Molecular Sensor (SSMS) and networks based on confined, birefringent CP heterostructures and CP based photonic bandgap (PBG) structures. A fully integrated SSMS structure is schematically depicted in Fig. 2. It consists of five basic elements labeled as such in the figure: (1) laser light source; (2) single or multiple optical confined CP heterostructure for the generation of coherent IR light (with either a broad IR wavelength output range or an externally controlled tuning range); (3) sensor area where selected beam(s) interacts with an interface, a gas volume, or an ambient; (4) detection unit(s); and (5) an analysis/discrimination unit with integrated feedback logic. Elements (2) and (3) can act collectively as a probe/sensor module. All of these components can be monolithically integrated on one substrate and organized into a hybrid structure, combining, for example, micro-bonded heterostructures. Alternatively, they may linked by waveguides or optical fibers to each other. The central pieces of the sensor are embedded birefringent CP heterostructures can be operated either as frequency agile coherent light source, or as an integral part of the SSMS detection system.

Figure 3 is a schematic that illustrates two of the possible multiple layered constructs that may be used in the architecture of an SSMS device. The frequency-agile optical parametric generator, based on graded nonlinear waveguide, is illustrated in Fig. 3a. All three participating waves propagate in spatially overlapping regions of the guide, which results in an efficient nonlinear interaction. Their cross extensions (in the growth direction) are indicated as the transversal dimensions of the corresponding waves. Phase matching is achieved by the corresponding choice of the direction of the optical axis of the crystal relative to the propagation direction. A significant advantage results by the use of refractive index graded layers that permit waveguided propagation of waves of different wavelengths in the same waveguide. In this way, one has the flexibility to either have nonlinear generated waves propagate in the same spatial region as the pump wave or, if desired, to separate them and force them to propagate in different waveguides.

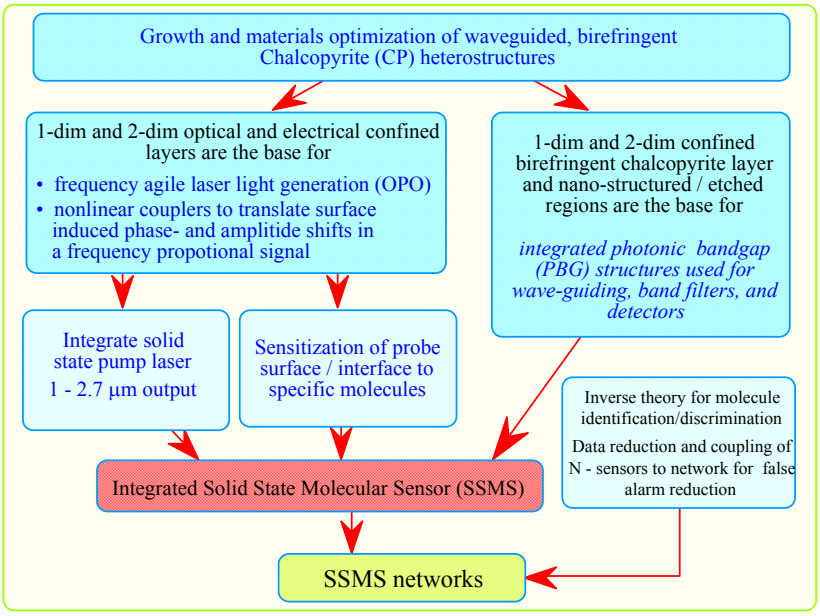

Figure 1

Development steps leading to integrated SSMS structures and networks of it.

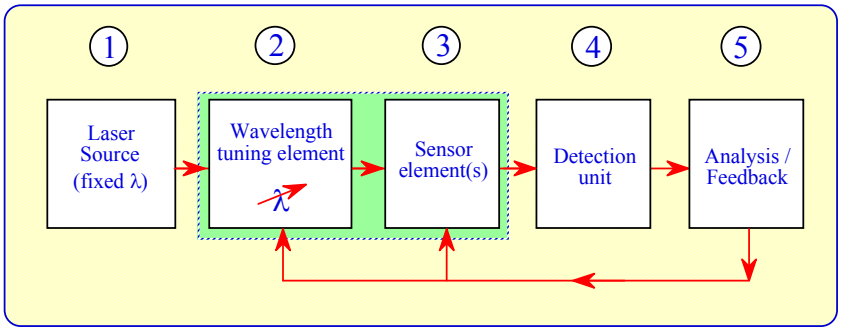

Figure 2.

Schematic of an integrated SSMS system.

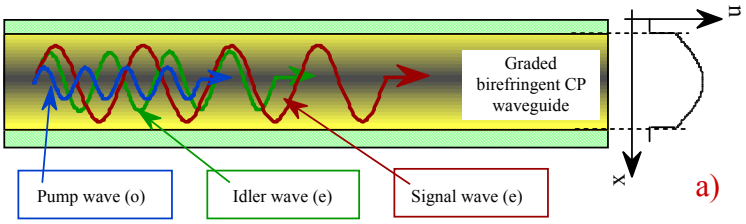

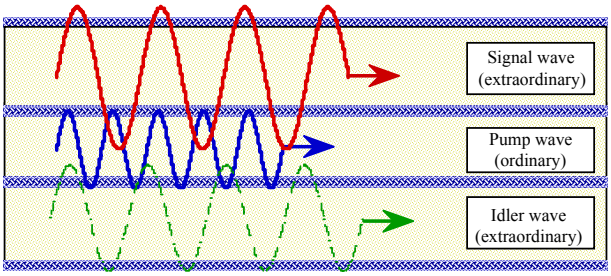

Figure 3.

(a) Optically confined single CP structure.

(b) Optically coupled, multiple CP heterostructures

An optical parametric generator is illustrated in Fig. 3b. Each layer of the triple heterosructure guides spatially separated

waves: the pump, the signal, and the idler. The three waveguides are single-mode, nonlinear, open resonators whose indices and thicknesses are chosen for the corresponding waves to propagate as the lowest modes. With the optical axis lying in the plane of the waveguide, phase matching is dependent on the angular orientation between it and the propagation vector of the wave. In addition, it is dependent on the orientation of the polarization of the pump wave with respect to the axis of the guide.

Figure 3b also illustrates the nonlinear interaction of the waves by "tunneling" between neighboring waveguides, i.e., the overlapping of their evanescent waves. Phase matching and the strength of the interactions depend explicitly on the thickness and geometry of the guide(s). Moreover, this structure has the added flexibility that phase matched coupling can occur between the various modes of the guide, which is absent in bulk materials.

The configurations illustrated Fig. 3 add flexibility to the design, manufacturing and operation of the integrated sensors, parametric light sources (fixed-frequency and tunable) and frequency-agile lasers.

Figure 4 demonstrates a detection/discrimination scheme based on the architecture of shown in Fig. 3b. The SSMS sensing area consist of three interacting waves each predominantly propagating in a separate guide. The spatial overlap of their evanescent waves penetrating into the adjacent guides and give rise to nonlinear interactions. Intuitively, it is expected that their interactions will be weak. However, this is compensated for by a high Q factor (low losses) of the waveguides. The principal advantage of this design is that the signal wave is separated from the pump and idler waves, which will dramatically decrease background scattering and noise. This is especially useful when using such devices as integrated sensors in the detection and discrimination of specific molecular targets. For such a use, the upper cladding in figure 4 can be chemically sensitized to allow absorption of specific, targeted molecules. Such a sensitized surface reaction layer will alter its optical dielectric properties upon reaction(s) with a specific molecule, antigen or antibody.

Surface absorbed molecules/structures can alter the EM wave interacting with the surface in two essential ways: (1) changing the differences in the dielectric functions forming the interface, which will induce a phase shift, and (2) absorption (preferably resonant) due to surface attachments, which will reduce the complex EM wave amplitude. Both effects will couple nonlinearly back to the underlying CP layer and alter the OPO process. An induced phase shift will alter the OPO frequency and a surface absorption loss will nonlinearly reduce the OPO generated laser output. An OPO frequency shift, though small, can be measured, e.g., by an optical beats method that is based on coherency of the signal wave. Accounting for the dielectric properties of the adsorbent molecules will be made by considering them as a composite and using a well-developed method given in a paper by Stockman, et al.[12]

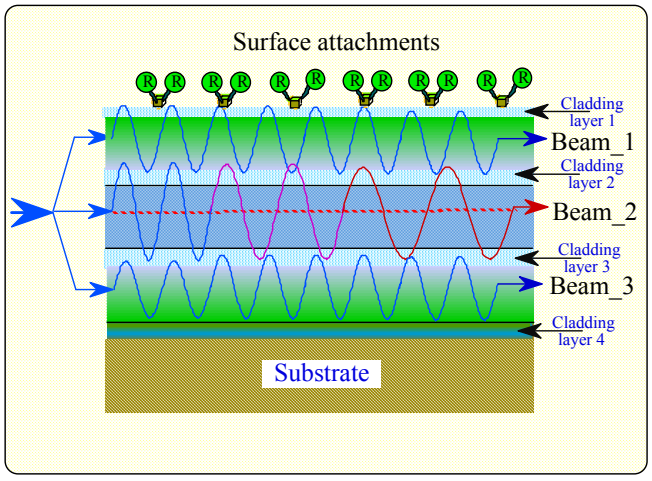

Figure 4.

Schematic of a differential sensor configuration using multiple layered linear/nonlinear optically confined heterostructures for high sensitive surface attachments characterization.

So far, the potential of ternary II-IV-V_2 bulk chalcopyrite (CP) compound semiconductor materials has been mostly explored in the context of their potential for nonlinear optical applications.[13-16] Although the CP semiconductors have electric, magnetic, and optical properties comparable or superior to their group IV, III-V or II-VI counterparts, for many applications CP semiconductors have advantages due to their lower crystal symmetry. Being optically birefringent and pleochroic, their optical and electro-optical properties are highly orientation dependent, thereby making them more sensitive to their environment. In principle, it will enable new capabilities in thin-film coupled-waveguide optoelectronic devices, where the possibility of controlling layer composition, thickness, and spacing is expected to lead to new levels of performance in linear and nonlinear devices. Their potential as ferromagnetic material systems compatible with III-V compound semiconductors opens new opportunities in exploring ferromagnetic nanocomposites. These are constructed by self-assembled techniques to control the size and distribution of magnetically active quantum-

dots.

Figure 5 depicts confined ferromagnetic CP structures either constructed utilizing self-assembly and engineered arrays of ferromagnetic QDs embedded in a birefringent active II-IV-V_2 layer. The active, birefringent II-IV-V_2 layer can be itself embedded in optical and/or electrical confinement layers[4].

The successful fabrication of such device structures will enable its applications as magneto-optical modulators, magneto-optic read-/write storage devices, magnetic spin-controlled frequency-agile laser sources, or spin-electronic devices. Figure 5b depicts a size- and distribution engineered assembly of magnetic quantum dots that are embedded in the birefringent active II-IV-V_2 layer(s). Such a structure can be embedded in optically confined cladding layers to form a nonlinear waveguided magnetic photonic crystal (MPC) structure, analogously to photonic crystals.[17] In addition to photonic band gap engineering, MPC structures will allow the exploration of linear and nonlinear optical device structures based on magneto-optical interactions in single quantum dots and coupled quantum dot arrays.

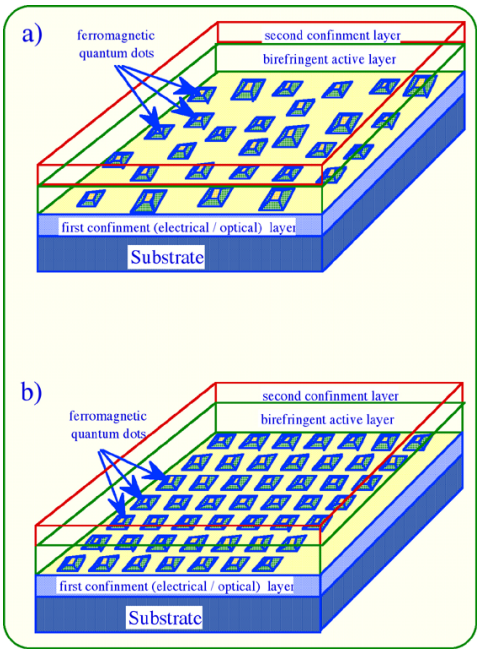

Figure 5:

Combination of nonlinear optical and magneto-optical materials properties for multifunctional device structures:

a) Self-assembled 3d-transition metal doped II-IV-V_2 quantum dots (QD) embedded in birefringent layer(s).

b) "***Magnetic Photonic Crystals:*** Built up by size and distribution engineered period assemblies of ferromagnetic quantum dots or quantum columns embedded in birefringent layer(s).

2.2. SSMS: Theoretical Background

Chalcopyrite compound semiconductors are being used to achieve wavelength agility through much of the infrared spectrum. However, many applications, such as optical parametric oscillation (OPO) and second harmonic generation (SHG), are limited by the phase-matching requirements of the bulk material. For example, $ZnGeP_2$ would make an excellent frequency doubler of 10.6μm radiation (yielding 5.3 μm radiation) but the phase matching conditions are difficult to achieve, which in turn places severe limitations on its conversion efficiency. The extraordinary wave index of refraction of $ZnGeP_2$ at 10.6 μm is almost exactly equal to the ordinary wave index of refraction at 5.3 μm making phase matching in bulk material marginal at best. This limitation, and corresponding limitations for other nonlinear processes, can be avoided by incorporating the $ZnGeP_2$, or other appropriate CP materials, in a waveguide structure. For example, the phase matching region for SHG can be considerably extended by coupling the pump into the guide in the fundamental, m = 0, mode and phase matching to the m = 2 mode of the second harmonic. Dimmock et al.[5] analyzed the phase matching conditions for SHG and OPO in birefringent nonlinear semiconductor waveguides and apply their results to the model system of $ZnGeP_2$ on a GaP substrate demonstrating the feasibility and efficient use of CP heterostrutures.

In order to achieve phase-matched conditions they considered that the optical axis of the $ZnGeP_2$ lies in the plane of the guide. In that case the angle between the direction of propagation of the wave in the guide and the optical axis of the guide material can be adjusted to achieve the phase matching condition. As shown below, this can be accomplished for both SHG and OPO for the example of $ZnGeP_2$ guides on GaP. Moreover, the waveguide geometry affords an additional opportunity for phase matching not available in bulk material. It is possible to couple radiation between

different modes of the guide. This will greatly extend the wavelength region over which phase-matched SHG can be achieved in a planar waveguide of $ZnGeP_2$.

To examine the specific examples of OPO and SHG Type I phase matching, we selected a $ZnGeP_2$ planar waveguide on a GaP substrate and a GaP cladding, the result of which is shown in Fig. 6. The optical axis of the $ZnGeP_2$ layer lies in the plane of the guide the optimum Type 1 non-linear coupling. For SHG Type I phase matching we considered that the guide is pumped in the TE mode with propagation at an angle Θ with respect to the optical axis of the $ZnGeP_2$.

The corresponding phase matching angles for bulk $ZnGeP_2$ are shown for comparison. These results show phase matching angles quite similar to those of bulk $ZnGeP_2$[18] as would be expected for a guide this thick. This simply shows that phased matched SHG and OPO should be readily obtainable in waveguides of $ZnGeP_2$ operating in the m = 0 mode. The applicability of the bulk indices for the waveguide will depend on the guide thickness, method of growth, degree of doping, lattice mismatch and internal strain. Bulk indices should be a good approximation for a well constructed 16 μm thick guide with reasonable lattice match as could be obtained with $ZnGeP_2$ on GaP. In Figure 7 the case where coupling into the guide occurs in one mode of the guide, the nonlinear process within the guide couples energy to another mode and coupling out of the guide occurs from the second mode is examined. Even though the calculation does not include details as of the strength of coupling, the estimated nonlinear coupling from the m = 0 to the m = 2 mode, is estimated to be as large as 20% of the coupling to the m = 0 mode of the guide for similar phase matching conditions. For the purpose of illustration, the case of SHG is considered, where the input wave is in the m = 0 mode with the second harmonic output considered in the m = 2 mode. Note that in this case phase matching for SHG can be obtained over wider wavelength region than for m = 0 to m = 0, or for bulk $ZnGeP_2$.

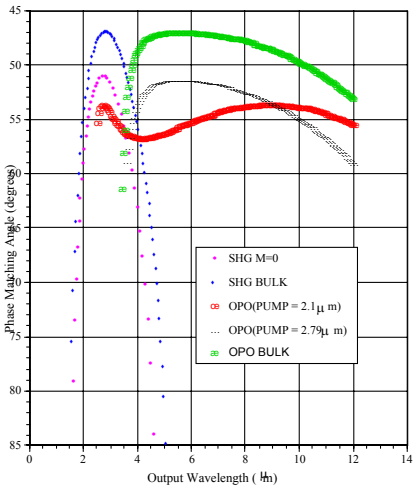

Figure 6. Calculated phase matching angles for SHG and OPO in a 16 μm $ZnGeP_2$ waveguide with a GaP substrate and cladding layer compared with similar curves for bulk material

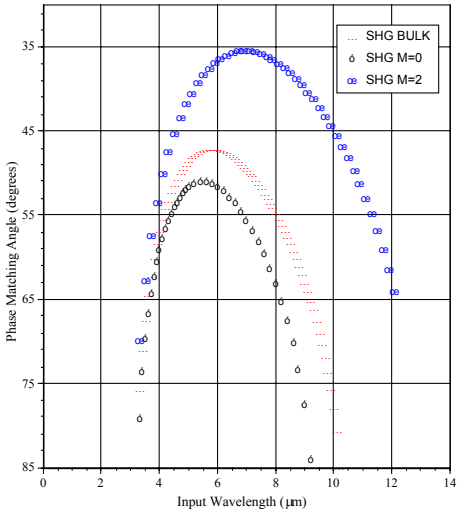

Figure 7. Calculated phase matching angles for SHG in the 16 μm $ZnGeP_2$ waveguide of Fig. 3b pumped in the m = 0 mode with output in the m = 2 mode compared to the m = 0 to m = 0 coupling of Fig. 3b and that of the bulk material.

2.3. II-IV-V_2 compound semiconductors

The ferromagnetic and birefringent properties of quantum dots (confined nanocomposites) and heterostructures can be explored in the following three material systems:

a) II-IV-phosphides: e.g. $(Zn_{1-x}Fr_x)(Ge_{1-y}Si_y)P_2$, $(Cd_{1-x}Fr_x)(Ge_{1-y}Si_y)P_2$, $(Cd_{1-x}Fr_x)(Sn_{1-y}Ge_y)P_2$; and

b) II-IV-arsenides: e.g. $(Zn_{1-x}Fr_x)(Ge_{1-x}Si_x)As_2$, $(Zn_{1-x}Fr_x)SnAs_2$, $(Cd_{1-x}Fr_x)(SiP_2$; and

c) II-IV-nitrides: e.g. $(Zn_{1-x}Fr_x)(Ge_{1-y}Si_y)N_2$,

where Fr denotes magnetic 3d-transition elements, such as Mn, Fe, Co, V, Cr, or Ni. The discovery of room-temperature ferromagnetism in Mn-doped $CdGeP_2$ and $ZnGeP_2$ chalcopyrite compounds[19-23] demonstrates the emerging potential of II-IV-V_2 chalcopyrite compound semiconductors for spintronic device applications. II-IV-V_2 semiconductors have an advantage over III-V materials because high concentrations of Mn can be incorporated into them due to the existence of a group II element. II-IV-V_2 compounds also have an advantage over II-VI materials due to

the similarity of their properties to other III-V materials. To date, published ferromagnetic research in II-IV-V materials has been limited primarily to $CdGeP_2$ and $ZnGeP_2$. The results of these studies have been promising, showing Mn concentrations of 20% and Curie temperatures around 300-320K. This combination of factors make II-IV-V_2 a perfect choice for multifunctional systems combing nonlinear optical and magneto-optical properties.

Figure 8 summarizes the lattice constants and band gap energies of several CP materials, together with the lattice constants and band gap energies of group IV-, III-V-, and II-VI compound semiconductors that can act as potential substrates as well as for the formation of electrical and optical confinements for 3d-transition element doped (Fr:II)-IV-V_2 nanocomposites and heterostructures. Figure 8a depicts the II-IV-phosphide and II-IV-arsenide compounds in relation to group IV-, III-V-compound semiconductor, while Fig. 8b shows the relation of some II-IV-N_2 compounds[24] to III-N compound semiconductors.

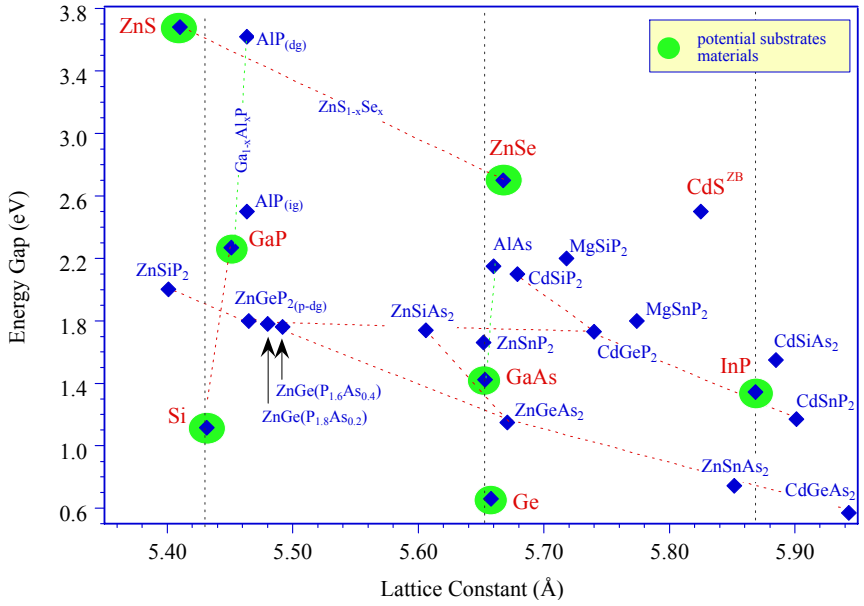

Figure 8:
Energy gaps and lattice constants for the selected II-IV-V_2 compound

(a) II-IV-P_2 and II-IV-As_2 compounds in relation to group IV, III-V and II-VI semiconductors (dg: direct gap, ig: indiect gap, p-dg: pseudo-direct gap).

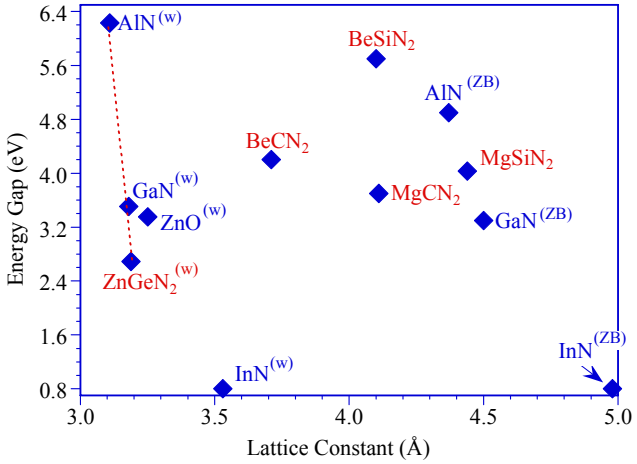

(b) II-IV-N_2 compounds in relation to group III-Nitrides
(w): wurtzite structure;
(ZB): zincblende structure.

The InN band gap is tentative assigned about 0.8 eV, noting that values between 1.5 eV and 0.7 eV are reported.

A comprehensive theoretical evaluation for potential ferromagnetic CP's for spintronic by density-functional theory was performed by Erwin et al.,[25] analyzing 64 possible combination in the II-IV-V_2 materials class. This evaluation also considered the availability of closely lattice-matched semiconductor substrates. For the formation of confined 3d transition element doped nanocomposites and heterostructures, the evaluation also has to take in account the availability of optical confinement layers as discussed previous.[4]

2.4. Materials selection consideration for SSMS device structures

Combining the requirements for optical confined birefringent compounds[4] with those compounds having the potential of room temperature (RT) ferromagnetism,[25] reduces the available material systems considerable as shown in Table 2. We included the group III-nitride compounds GaN and InN due to their strong potential to act not only as a ferromagnetic host, but also as template for confined II-V-N_2 nanocomposites and heterostructures.

Table 2. Potential multifunctional material combinations for SSMS devices

	3d-transition element (Fr) doped semiconductor compound	Lattice-matched substrates	Confinement layers
Potential of having RT ferromagnetism	GaN	Sapphire, ZnO, AlN	$Ga_{1-x}Al_xN$
	InN	Sapphire, ZnO, AlN	$Ga_{1-x}In_xN$
Birefringent II-V-N_2 with potential of having RT ferromagnetism	$Zn(Ge_{1-x}Si_x)N_2$	wurtzite GaN, SiC, Sapphire	$Ga_{1-x}Al_xN$,
	(Mg or Be)SiN_2	zincblende $Ga_{1-x}Al_xN$	??
Birefringent II-V-P_2 with potential of having RT ferromagnetism	$Zn(Ge_{1-x}Si_x)P_2$	GaP and Si	$Ga_{1-x}Al_xP$
	$(Cd_{1-x}Zn_x)$ Ge P_2	GaAs, ZnSe	$Ga_{1-x}Al_xAs$
	$ZnSnP_2$	GaAs, ZnSe	$Ga_{1-x}Al_xAs$
	$Cd(Ge_{1-x}Sn_x)P_2$	InP	CdS
Birefringent II-V-As_2 with potential of having RT ferromagnetism	$Zn(Ge_{1-x}Si_x)As_2$	GaAs, ZnSe	$Ga_{1-x}Al_xAs$

The growth of group III-V semiconductor device structures has been proven most efficient by metal-organic chemical vapor deposition (MOCVD). It has been successfully applied to the growth of $(Ga_{1-x}Al_y)As$, $(Ga_{1-x}In_y)P$ and $(Ga_{1-y}Al_y)N$ device structures. Only the growth of indium rich $(In_{1-x}Ga_x)N$ alloys becomes a major challenge due to stoichiometric instabilities and low dissociation temperatures.[26] As successfully demonstrated for the CP compound $ZnGeP_2$, [27,28] the growth by MOCVD should be possible for most of the II-IV-P_2 and II-IV-As_2 alloys, utilizing a main-stream growth technology. SSMS devices operating on the near- and mid-infrared regime favor the exploration of optical confined $Zn(Ge_{1-y}Si_y)P_2$ heterostructures as well as the exploration of 3d-transition element doped $Zn(Ge_{1-y}Si_y)P_2$ QDs and nanocomposites.

The growth of The $Zn(Ge_{1-x}Si_x)N_2$ by MOCVD, using germane and silane as group IV sources, ammonia as nitrogen source and tetraethyl zinc as group II source has been also demonstrated.[29] Since room-temperature ferromagnetism has been already demonstrated for Mn doped GaMnN epilayers,[30,31] the coupling of confined birefringent $Zn(Ge_{1-x}Si_x)N_2$ with ferromagnetic group III-nitride are very promising for unique electro- / magneto-optical device structures. The fabrication and study of such systems will be crucial for the validation and understanding of electromagnetic wave propagation in ferromagnetically, birefringent waveguides.

3. CONCLUSION

The design and construction for a unique Solid-State Molecular Sensor (SSMS) system is discussed. SSMS structure are based on confined, birefringent and/or magnetic active II-IV-V_2 compound semiconductors, which potential applications for compact ultra-sensitive chemicals and biological molecule sensors, nonlinear optical modulators, QD lasers, magneto-optical switches, detectors, and spin electronic devices. Utilizing the nonlinear optical interactions in optically confined II-IV-V_2 heterostructures as well as magneto-optical interactions of ferromagnetic and nonlinear optical coupled structures, provide for high sensitivity and discrimination capability of SSMS devices. $Zn(Ge_{1-y}Si_y)P_2$ and $Zn(Ge_{1-x}Si_x)N_2$ are CP materials systems that are suitable for such a SSMS system. The spectral range of operation would extend from 500 nm to 10 μm, allowing for the discrimination and identification of almost all molecular structures in a probed medium or attached at a probed interface/surface, using resonant phase- and/or amplitude sensitive detection.

Both systems will allow for the construction of optically confined birefringent heterostructures, closely lattice-matched onto readily available group IV, III-V or II-VI substrates. Waveguided birefringent heterostructures based on the

$Zn(Ge_{1-x}Si_x)P_2$ and $Zn(Ge_{1-x}Si_x)N_2$ will have the potential advantage of a monolithic integrated all optical sensor. At present, however, little is know about the linear and nonlinear optical properties of these material system. The development of multi-functional $Ga_{1-x}Al_xN$:$Zn(Ge_{1-x}Si_x)N_2$ devices structures is favorable for sensors requiring a higher operation temperatures, a larger optical transparency window, and of being robust against radiation damage.

The theoretical analysis of phase matching in these nonlinear, birefringent heterostructures has been applied to the specific guide material $ZnGeP_2$ on a GaP substrate. The results showed that this structure has the added flexibility that phase matched coupling can occur between the various modes of the guide, where the coupling is a function of the guide thickness. These added degrees of freedom will allow for high gain under conditions where it is difficult or impossible to achieve in bulk material. The results also indicate, among other things, that $ZnGeP_2$ waveguides with harmonic output in the m = 2 mode can be used for efficient SHG from input radiation around 10.6 μm where bulk efficiencies in this wavelength range are too small to be useful. Indeed, the realization of such a structure would pave the way for a myriad of novel opto-electronic devices.

REFERENCES

1 US Patent No. **6,442,319**, "Chalcopyrite Based Nonlinear Waveguided Heterostructure Devices and Operating Methods", N. Dietz and K.J. Bachmann, Aug. 27, 2002.

2 US Patent No. **6,834,149**, "Optically Confined Birefringent Chalcoprite Heterostructure Devices and Operating Methods," N. Dietz, F. Madarasz, and D. Krivoshik, December 22, 2004.

3 US Patent Application No. **20/694,123**, "Room-Temperature Ferromagnetic Nanocomposites and Hetersostructures Based on (Fr:II)-IV-V_2 Compounds," N. Dietz and F. Madarasz, October 27, 2003.

4 N. Dietz and F. L. Madarasz, "Chemical and Biological Sensors based on optically confined birefringent chalcopyrite heterostructures," Mater. Sci. & Eng. B, Vol **97**(2) pp. 182-195 (2003).

5 J. O. Dimmock, F. L. Madarasz, N. Dietz and K. J. Bachmann, "A theoretical analysis of phase matched SHG and OPO in birefringent semiconductor waveguides," Applied Optics **40**(9), pp. 1438-1441 (2001).

6 "Chemical and Biochemical Sensing with Optical Fibers and Waveguides," ed. Gilbert Boisdé and Alan Harmer, ISBN 0-89006-737-6; Artech House, Inc, Norwood, MA 02062 (1996).

7 P. A. Budni, K. Ezzo, P. G. Schunemann, S. Minnigh, J. C. McCarthy and T. M. Pollak, "2.8 micron pumped optical parametric oscillation in ZnGeP2," OSA Proceedings on Advanced Solid-State Lasers. Vol.10, Proceedings of the Topical Meeting, pp. 335-8 (1991).

8 P. A. Budni, P. G. Schunemann, M. G. Knights, T. M. Pollak and E. P. Chicklis, "Efficient, high average power optical parametric oscillator using $ZnGeP_2$," OSA Proceedings on Advanced Solid-State Lasers. Vol.13. Proceedings of the Topical Meeting, pp. 380-3 (1992).

9 Y. M. Andreev, P. P. Geiko, G. M. Krekov and O. A. Romanovskii, "Detection of trace concentration of some simple pollutants in Tomsk," Proceedings of the SPIE Vol. **1811**, 367-70 (1992).

10 K. Stoll, J.-J. Zondy and O. Acef, "Fourth-harmonic generation of a continuous-wave CO_2 laser by use of an $AgGaSe_2$/ $ZnGeP_2$ doubly resonant device," Optics Letters **22**, pp. 1302-1304 (1997)

11 N. P. Barnes, K. E. Murray, M. G. Jani, P. G. Schunemann and T. M. Pollak, "$ZnGeP_2$ parametric amplifier," J. Opt. Soc. Am. B **15**(1) pp. 232-238 (1998).

12 M.I.Stockman, K.B.Kurlayev, and T.F.George, "Linear and Nonlinear Optical Susceptibilities of Maxwell Garnett Composites: Dipolar Spectral Theory," Phys. Rev. B **60**(24), pp. 17071-17083 (1999).

13 Ternary Chalcopyrite Semiconductors: Growth, Electronic Properties, and Applications, ed. J. L. Shay and J. H. Wernick, Oxford, New York, Pergamon Press [1975].

14 M. M. Tilleman and A, Englander, "Optimal frequency doubling of a transferred-electron amplifier CO_2 laser," Optical Engineering **39**(3), pp. 758-762 (2000).

15 S. N. Rashkeev, S. Limpijumnong and W. R. L. Lambrecht, "Second-harmonic generation and birefringence of some ternary pnictide semiconductors," Phys. Rev. B. **59**(2), pp. 2737 - 2748 (1999).

16 K. L. Vodopyanov, F. Ganikhanov, J. P. Maffetone, I. Zwieback, and W. Ruderman, "$ZnGeP_2$ optical parametric

oscillator with 3.8< 12.4 μm tunability," Optics Letters **25**(11) pp. 841-843 (2000).

[17] "Photonic crystals: molding the flow of light," ed. R. D. Meade, J. D. Joannopoulos, J. N. Winn, Princeton University Press, ISBN: 0691037442, (1995).

[18] "Emergence of chalcopyrites as nonlinear optical materials," M. C. Ohmer and R. Pandey, (eds.), Materials Reseach Bulletin, Vol. **23**(7) 1998.

[19] Yu-Jun Zhao, W. T. Geng, A. J. Freeman, T. Oguchi, "Magnetism of chalcopyrite semiconductors: $Cd_{1-x}Mn_xGeP_2$", Phys. Rev. B **63**, pp. 201202-4 (2001).

[20] G. A. Medvedkin, K. Hirose, T. Ishibashi, T. Nishi, V. G. Voevodin, and K. Sato, "New magnetic materials in $ZnGeP_2$-Mn chalcopyrite system," J. Crystal Growth, **236**(4) pp. 609-612 (2002).

[21] K. Sato, G. A. Medvedkin, T. Ishibashi, S. Mitani, K. Takanashi, Y. Ishida, D. D. Sarma, J. Okabayashi, A. Fujimori, T. Kamatani and H. Akai, "Novel Mn-doped chalcopyrites,",J. Phys. Chem. Solids, 4(9-10), pp. 1461-1468 (2003).

[22] V.V. Popov, G.A. Medvedkin, "Hole transport anomaly in high-T_C ferromagnet $(Zn,Mn)GeP_2$," Solid State Communications, **132**(8) pp. 561-565 (2004).

[23] H. Yi and Hy. Park, "Electronic structure and magnetism of chalcopyrite semiconducting $CdGeP_2$:Cr," Physica B **359-361** pp. 1466-1468 (2005).

[24] A. G. Petukhov, W. R. L. Lambrecht, and B. Segall, "Electronic structure of wide-band-gap ternary pnictides with the chalcopyrite structure," Phys. Rev. B **49**, pp. 4549–4558 (1994).

[25] Steven C. Erwin, Igor Zuticacute, "Tailoring ferromagnetic chalcopyrites," Nature Materials **3**(6) pp. 410-414 (2004).

[26] *"Indium-nitride growth by HPCVD: Real-time and ex-situ characterization,"* N. Dietz, book chapter in "GaN-based Materials: Epitaxy and Characterization", ed. Z.C. Feng, Imperial College Press (ICP) pp. 1-31 (2005).

[27] G.C. Xing, K.J. Bachmann, G.S. Solomon, J.B. Posthill and M.L. Timmons, "Organometallic Chemical Vapor Deposition of Epitaxial $ZnGeP_2$ Films on (001) GaP Substrates," J. Crystal Growth **94**(2) pp. 381-386 (1989).

[28] G.C. Xing and K.J. Bachmann, "GaP/$ZnGeP_2$ Multiple Heterostructure," J. Crystal Growth **147**(1/2), pp. 35-8 (1995).

[29] S. J. Pearton, M. E. Overberg, C. R. Abernathy, N. A. Theodoropoulou, A. F. Hebard, S. N. G. Chu, A. Osinsky, V. Fuflyigin, L. D. Zhu, A. Y. Polyakov, R. G. Wilson, "Magnetic and structural characterization of Mn-implanted, single-crystal $ZnGeSiN_2$," J. Appl. Phys. **92**(4) pp. 2047-2051 (2002).

[30] M. Kane, A. Asghar, A.M. Payne, C.R. Vesta, M. Strassburg, J. Senawiratne, Z J. Zhang, N. Dietz, C. Summers, I.T. Ferguson, "Magnetic and optical properties $Ga_{1-x}Mn_xN$ Grown by Metalorganic Chemical Vapor Deposition," Semicond. Sci. Technol. **20** L5–L9 (2005).

[31] M.H. Kane, M. Strassburg, A. Asghar, Q. Song, S. Gupta, J. Senawiratne, C. Hums, U. Haboeck, A. Hoffmann, D. Azamat, W. Gehlhoff, N. Dietz, Z.J. Zhang, C.J. Summers, I.T. Ferguson, "Multifunctional III-nitride dilute magnetic semiconductor epilayers and nanostructures as a future platform for spintronic devices," Proc. SPIE Vol. **5732** pp. 389-400 (2005).